Galaxy Cluster Gas Mass Fraction and Hubble Parameter versus Redshift Constraints on Dark Energy

Lado Samushia[1,2,3], Gang Chen[4,5], and Bharat Ratra[1,6]

ABSTRACT

Galaxy cluster gas mass fraction versus redshift data (Allen et al. 2004) and Hubble parameter versus redshift data (Simon et al. 2005) are used to jointly constrain dark energy models. These constraints favor the Einstein cosmological constant limit of dark energy but do not strongly rule out slowly-evolving dark energy.

Subject headings: cosmology: cosmological parameters — cosmology: observations — X-rays: galaxies

1.   Introduction

Type Ia supernova apparent magnitude versus redshift data now favor nonzero dark energy at about four standard deviations (see, e.g., Clocchiatti et al. 2006; Astier et al. 2006; Riess et al. 2007; Davis et al. 2007). Consistent with this, cosmic microwave background anisotropy measurements indicate that the Universe is spatially flat (see, e.g., Podariu et al. 2001; Durrer et al. 2003; Page et al. 2003; Spergel et al. 2007, if the dark energy density is assumed to be a constant, see, e.g., Wright 2006; Wang & Mukherjee 2007), and, in conjunction with the low observed nonrelativistic matter density (see, e.g., Chen & Ratra 2003b;

[1]Department of Physics, Kansas State University, 116 Cardwell Hall, Manhattan, KS 66506

[2]National Abastumani Astrophysical Observatory, 2A Kazbegi Ave, GE-0160 Tbilisi, Georgia

[3]email: lado@phys.ksu.edu

[4]Institute for Astronomy, 2680 Woodlawn Drive, Honolulu, HI 96822

[5]email: gchen@ifa.hawaii.edu

[6]email: ratra@phys.ksu.edu

Spergel et al. 2007), imply that dark energy (DE) accounts for ~ 70 % of the Universe's energy budget.

A number of explanations have been proposed for the DE phenomena. DE might be a cosmological constant (Peebles 1984) or it could be a dynamic scalar field with negative pressure (Peebles & Ratra 1988).[1] For recent dark energy reviews see, e.g., Peebles & Ratra (2003), Padmanabhan (2005), Copeland et al. (2006), and Nobbenhuis (2006).

Since different DE models make different predictions for the expansion history of the Universe and for the growth of perturbations, DE model parameters can be constrained by using available cosmological observations. Observations such as Type Ia supernova (SNIa) apparent luminosity versus redshift (see, e.g., Nesseris & Perivolaropoulos 2006; Jassal et al. 2006; Barger et al. 2007); cosmic microwave background anisotropy (see, e.g., Mukherjee et al. 2003; Spergel et al. 2007); the angular size versus redshift relation for quasars and radio sources (see, e.g., Chen & Ratra 2003a; Podariu et al. 2003; Daly & Djorgovski 2006); strong gravitational lensing by a foreground galaxy or cluster of galaxies (see, e.g., Chae et al. 2004; Alcaniz et al. 2005; Fedeli & Bartelmann 2007); and various large-scale structure measurements (see, e.g., Seljak et al. 2005; Tegmark et al. 2006; Percival et al. 2007), including baryon acoustic peak measurements (see, e.g., Eisenstein et al. 2005; Wang 2006; Doran et al. 2007; Parkinson et al. 2007), and galaxy cluster number counts (see, e.g., Voit 2005; Younger et al. 2005), may be used to constrain model parameters.

Since most observables depend on combinations of cosmological parameters rather then on just a single parameter, a single data set can not provide strong constraints. To get around this it is important to consider many different cosmological tests. This allows for consistency checks and might also allow for identification of systematic effects present in a particular data set. Combining data sets with constraints that are orthogonal to each other in parameter space results in significantly tighter constraints.

In this paper we use galaxy cluster gas mass fraction versus redshift data (Allen et al. 2004, also see Sasaki 1996; Pen 1997) and Hubble parameter versus redshift data (Simon et al. 2005, also see Jimenez & Loeb 2002) to jointly constrain parameters of three different dark energy models. The first model we study is the cosmological constant dominated cold dark matter model (ΛCDM) with redshift-independent cosmological constant energy density parameter Ω_Λ. We also consider the XCDM parametrization of dark energy, where dark energy is taken to be a fluid with an equation of state that relates pressure $p_x = \omega_x \rho_x$ to the energy density ρ_x, where ω_x is a negative constant (this is only an approximate parametrization of

---

[1]Alternatively, it could be that general relativity needs to be modified on very large scales (see, e.g., Wang et al. 2007; Movahed et al. 2007; Tsujikawa 2007; Elizalde et al. 2007).

dark energy). Thirdly, we consider a slowly-rolling dark energy scalar field model (ϕCDM) in which the scalar field ϕ has potential energy density $V(\phi) \propto \phi^{-\alpha}$, where α is a nonnegative constant (Peebles & Ratra 1988; Ratra & Peebles 1988). For the ϕCDM and XCDM cases we only consider spatially-flat spacetimes, while in the ΛCDM model spatial curvature is allowed to be nonzero. XCDM and ϕCDM reduce to the time-independent dark energy ΛCDM model when $\omega_\mathrm{x} = -1$ and $\alpha = 0$, respectively. In this paper we jointly analyze both data sets and derive constraints on the nonrelativistic matter density parameter Ω_m and a parameter p that describes the DE. The parameter p is Ω_Λ for ΛCDM, ω_x for XCDM, and α for ϕCDM.

The galaxy cluster gas mass fraction versus redshift data has been used to constrain parameters of the ΛCDM, XCDM and ϕCDM models (Allen et al. 2004; Chen & Ratra 2004). These data provide tight constraints on Ω_m. Rapetti et al. (2005) used the galaxy cluster data in combination with CMB anisotropy and SNIa measurements to constrain dark energy evolution. For the XCDM model, assuming a time-independent equation of state, they set tight limits, $\omega_\mathrm{x} = -1.05^{+0.10}_{-0.12}$, while more generally they found no significant evidence for evolution in the dark energy equation of state. Wilson et al. (2006) used these data in combination with SNIa data and found that the joint constraints were significantly tighter then those derived from either data set alone; the combined analysis favored the ΛCDM model but did not strongly rule out slowly-evolving dark energy. Alcaniz & Zhu (2005) used the galaxy cluster data and SNIa data (along with priors on the Hubble parameter and the baryonic matter density) to jointly constrain brane world models. This data set has been used in conjunction with Fanaroff-Riley type IIb radio galaxy angular size distance measurements to put an upper limit on the amplitude of non-Riemannian terms during the late stages of the Universe's evolution (Puetzfeld et al. 2005). Galaxy cluster gas mass fraction data have also been used to constrain other dark energy models (see, e.g., Chang et al. 2006; Zhao et al. 2006).

The $H(z)$ data were used by Samushia & Ratra (2006) to constrain cosmological parameters in the ΛCDM, XCDM and ϕCDM models, but a computational error was made when cosmological parameter confidence contours were calculated. Sen & Scherrer (2007) used these data to constrain the evolution of an arbitrary dark energy component that satisfies the weak energy condition, in spatially-flat models. The $H(z)$ data set has also been used to constrain a number of interacting dark energy models (Wei & Zhang 2007a,b; Zhang & Zhu 2007). In combination with CMB anisotropy measurements and SNIa data it has been used to constrain the Chaplygin gas model (Wu & Yu 2007) as well as cosmological models motivated by higher dimensional theories (Lazkoz & Majerotto 2007).

In this paper we present corrected cosmological parameter constraints for the $H(z)$

data. We also provide joint constraints on the ΛCDM, XCDM, and ϕCDM models from the $H(z)$ and galaxy cluster gas mass fraction versus redshift data. In Sec. 2 we outline our computational method. Results are presented and discussed in Sec. 3.

2. Computation

We use the Allen et al. (2004) measurements of gas mass fractions for 26 relaxed rich clusters in the redshift range $0.08 < z < 0.89$. The cluster baryon mass is dominated by the gas. In relaxed rich clusters the baryon fraction should be independent of redshift. The cluster baryon fraction value depends on the angular diameter distance, so the correct cosmological parameter values place clusters at the right angular diameter distance to ensure the redshift independence of the cluster baryon fraction. We follow Chen & Ratra (2004) and compute the two dimensional likelihood function $L^G(\Omega_{\mathrm{m}}, p)$ for each of the three DE models. When computing $L^G(\Omega_{\mathrm{m}}, p)$ we marginalize over the Gaussian uncertainties in the bias factor b, in the Hubble constant h (in units of $100 \mathrm{\ km\,s}^{-1}\mathrm{Mpc}^{-1}$), and in the baryonic matter density parameter Ω_{b}. Following Allen et al. (2004), we use $b = 0.824 \pm 0.089$ (one standard deviation error) for the bias factor. To reflect the range of uncertainties, we use two sets of values for h and $\Omega_{\mathrm{b}}h^2$. One set is $\Omega_{\mathrm{b}}h^2 = 0.014 \pm 0.004$ (one standard deviation error, Peebles & Ratra 2003) and $h = 0.68 \pm 0.04$ (one standard deviation error, Gott et al. 2001; Chen et al. 2003). The other is from the WMAP three-year data, $\Omega_{\mathrm{b}}h^2 = 0.0228 \pm 0.0007$ and $h = 0.73 \pm 0.03$ (one standard deviation errors, Spergel et al. 2007).

The second data set we use are the nine Simon et al. (2005) measurements of the Hubble parameter in the redshift range $0.09 < z < 1.75$. Following Samushia & Ratra (2006) we compute a two dimensional likelihood function $L^H(\Omega_{\mathrm{m}}, p)$ for each DE model. $H(z)$ is not sensitive to the bias factor or baryonic matter density, but we still have to account for uncertainties in the Hubble constant. For the Hubble constant prior probability distribution function we use the same set of values as in the previous paragraph.

To derive joint constraints, for each DE model we define the joint likelihood function $L(\Omega_{\mathrm{m}}, p) = L^G(\Omega_{\mathrm{m}}, p)L^H(\Omega_{\mathrm{m}}, p)$. From the joint likelihood function we compute 1, 2, and 3 σ confidence contours, as the contours that enclose 68, 95, and 99 % of the total probability.

3. Discussion and Conclusion

Figures 1 to 3 show cosmological parameter confidence contours for the ΛCDM, XCDM and ϕCDM models for the two sets of $\Omega_{\mathrm{b}}h^2$ and h priors.

Figure 1 shows constraints on the ΛCDM model. The galaxy cluster gas mass fraction data place a good constraint on Ω_m (< 0.35 at 3 σ), while the $H(z)$ data constrain a linear combination of Ω_m and Ω_Λ. The joint likelihood functions peak near spatially-flat models.

Figure 2 shows the constraints for the XCDM parametrization. The joint constraints favor the region of parameter space near the $\omega_x = -1$ line which corresponds to spatially-flat ΛCDM models.

Figure 3 is for the ϕCDM model. The joint likelihoods peak on the $\alpha = 0$ line which corresponds to the spatially-flat ΛCDM model. However, values of α as high as 4 or 5 are allowed at 3 σ.

The galaxy cluster gas mass fraction data is more restrictive than the $H(z)$ data. When they are combined the $H(z)$ data shifts the constraints to slightly higher values of Ω_m than for the galaxy cluster gas mass fraction data set alone. A spatially-flat cosmological model with a cosmological constant term with $\Omega_\Lambda \simeq 0.7$ is a good fit to the joint data in all six cases considered here. This is consistent with results based on other measurements, see, e.g., Rapetti et al. (2005), Wilson et al. (2006), and Davis et al. (2007).

Hubble parameter versus redshift data is expected to increase by an order of magnitude in the next few years. In combination with new galaxy cluster gas mass fraction, SNIa, and CMB measurements, this will significantly better constrain dark energy models.

REFERENCES

Alcaniz, J. S., Dev, A., & Jain. D. 2005, ApJ, 627, 26

Alcaniz, J. S., & Zhu, Z.-H. 2005, Phys. Rev. D, 71, 3153

Allen, S. W., et al. 2002, MNRAS, 353, 457

Astier, P., et al. 2006. A&A, 447, 31

Barger, V., Gao, Y., & Marfatia, D. 2007, Phys. Lett. B, 648, 127

Copeland, E. J., Sami, M., & Tsujikawa, S. 2006, Int. J. Mod. Phys.D, 15, 1753

Chae, K.-H., Chen, G., Ratra, B., & Lee, D. W. 2004, ApJ, 607, 71

Chang, Z., et al. 2006, Phys. Lett. B, 633, 14

Chen, G., Gott, J. R., & Ratra, B. 2003, PASP, 115, 1269

Chen, G., & Ratra, B. 2003a, ApJ, 582, 586

Chen, G., & Ratra, B. 2003b, PASP, 115, 1143

Chen, G., & Ratra, B. 2004, ApJ, 612, 1

Clocchiatti, A., et al. 2006, ApJ, 642, 1

Daly, R. A., & Djorgovski, S. G. 2006, arXiv:astro-ph/0609791

Davis, T. M., et al. 2007, arXiv:astro-ph/0701510

Doran, M., Stern, S., & Thommes, E. 2007, J. Cosmology Astropart. Phys., 0704 , 015

Durrer, R., Novosyadlyj, B., & Apunevych, S. 2003, ApJ, 583, 33

Eisenstein, D. J., et al. 2005, ApJ, 633, 560

Elizalde, E., et al. 2007, arXiv:0705.1211

Fedeli, C., & Bartelmann, M. 2007, A&A, 461, 49

Gott, J. R., Vogeley, M. S., Podariu, S., & Ratra, B. 2001, ApJ, 549, 1

Jassal, H. K., Bagla, J. S., & Padmanabhan, T. 2006, arXiv:astro-ph/0601389

Jimenez, R., & Loeb, A. 2002, ApJ, 573, 37

Lazkoz, R., & Majerotto, E. 2007, arXiv:0704.2606

Movahed, M. S., Baghram, S, & Rahvar, S. 2007, arXiv:0705.0889

Mukherjee, P, et al. 2003, Int. J. Mod. Phys. A, 18, 4933

Nesseris. S., & Perivolaropoulos, L. 2006, Phys. Rev. D, 75, 023517

Nobbenhuis, S. 2006, arXiv:gr-qc/0609011

Padmanabhan, T. 2005, Curr. Sci., 88, 1057

Page, L., et al. 2003, ApJS, 148, 223

Parkinson, D., et al. 2007, MNRAS, 377, 185

Peebles. P. J. E. 1984, ApJ, 284, 439

Peebles, P. J. E., & Ratra, B. 1998, ApJ, 325, 17

Peebles, P. J. E., & Ratra, B. 2003, Rev. Mod. Phys., 75 , 559

Pen, U. L. 1997, New A, 2, 309

Percival, W. J., et al. 2007, ApJ, 657, 645

Podariu, S., Daly, R. A., Mory, M. P., & Ratra, B. 2003, ApJ, 584, 577

Podariu, S., et al. 2001, ApJ, 559 , 9

Puetzfeld, D., Pohl, M., & Zhu, Z.-H. 2005, ApJ, 619, 657

Rapetti, D., Allen, S., & Weller, J. 2005, MNRAS, 360, 555

Ratra, B,. & Peebles, P. J. E. 1988, Phys. Rev. D, 37, 3406

Riess, A. G., et al. 2007, ApJ, 659, 98

Samushia, L., & Ratra, B. 2006, ApJ, 650, 5

Sasaki, S. 1996, PASJ, 48, 119

Seljak, U., et al. 2005, Phys. Rev. D, 71, 103515

Sen, A. A., & Scherrer, R. J. 2007, arXiv:astro-ph/0703416

Simon, J., Verde, I., & Jimenez, R. 2005, Phys. Rev. D, 71, 123001

Spergel, D. N., et al. 2003, ApJS, 148, 175

Spergel, D. N., et al. 2007, arXiv:astro-ph/0603449

Tegmark, M., et al. 2006, Phys. Rev. D, 74, 123507

Tsujikawa, S. 2007, arXiv:0705.1032

Voit, G. M. 2005, Rev. Mod. Phys., 77, 207

Wang, S., Hui, L., May, M., & Haiman, Z. 2007, arXiv:0705.0165

Wang, Y. 2006, ApJ, 647, 1

Wang, Y., & Mukherjee, P. 2007, arXiv:astro-ph/0703780

Wei, H., & Zhang, S. N. 2007a, Phys. Lett. B, 644, 7

Wei. H., & Zhang, S. N. 2007b, arXiv:0704.3330

Wilson, K., Chen. G., & Ratra, B. 2007, Mod. Phys. Lett. A, 21, 2197

Wright, E. L. 2006, arXiv:astro-ph/0603750

Wu, P., & Yu, H., 2007 Phys. Lett. B, 644, 16

Younger, J. D., Bahcall, N. A., & Bode, P. 2005, ApJ, 622, 1

Zhang, H., & Zhu, Z.-H. 2007, arXiv:astro-ph/0703245

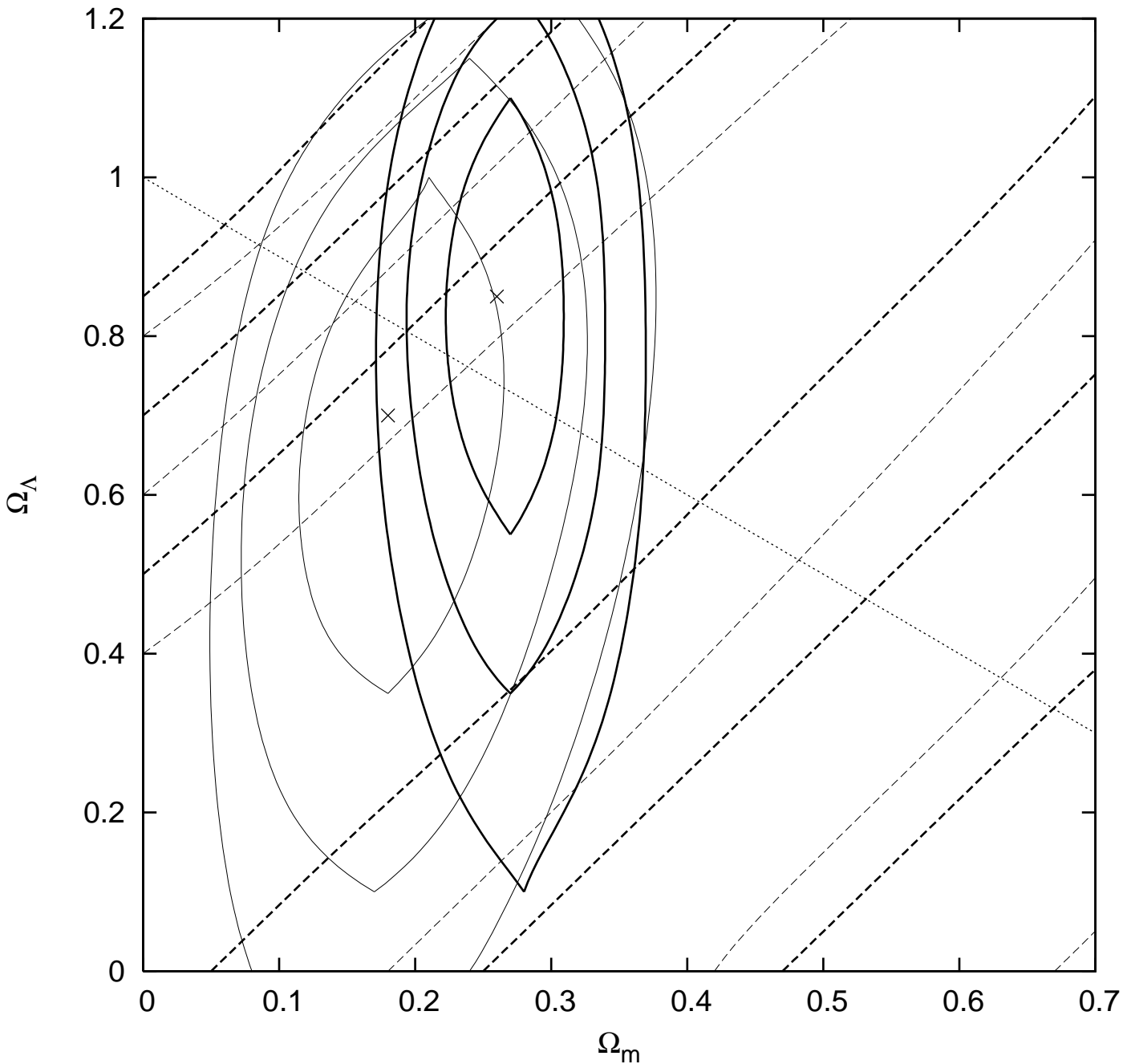Zhao, G. D., Xia, J.-Q., Feng, B., & Zhang, X. 2006, astro-ph/0603621

Fig. 1.— 1, 2, and 3 σ confidence level contours for the ΛCDM model. Dashed lines denote constraints from Hubble parameter versus redshift data, while solid lines show the joint constraints (the crosses indicate the maximum likelihood points). The diagonal dotted line corresponds to spatially-flat ΛCDM models. Thick lines correspond to the $h = 0.73 \pm 0.03$ and $\Omega_{\mathrm{b}} h^2 = 0.022 \pm 0.0007$ priors (maximum likelihood is at $\Omega_{\mathrm{m}} = 0.26$ and $\Omega_{\Lambda} = 0.85$), while thin lines are for $h = 0.68 \pm 0.04$ and $\Omega_{\mathrm{b}} h^2 = 0.014 \pm 0.04$ (maximum likelihood is at $\Omega_{\mathrm{m}} = 0.18$ and $\Omega_{\Lambda} = 0.70$).
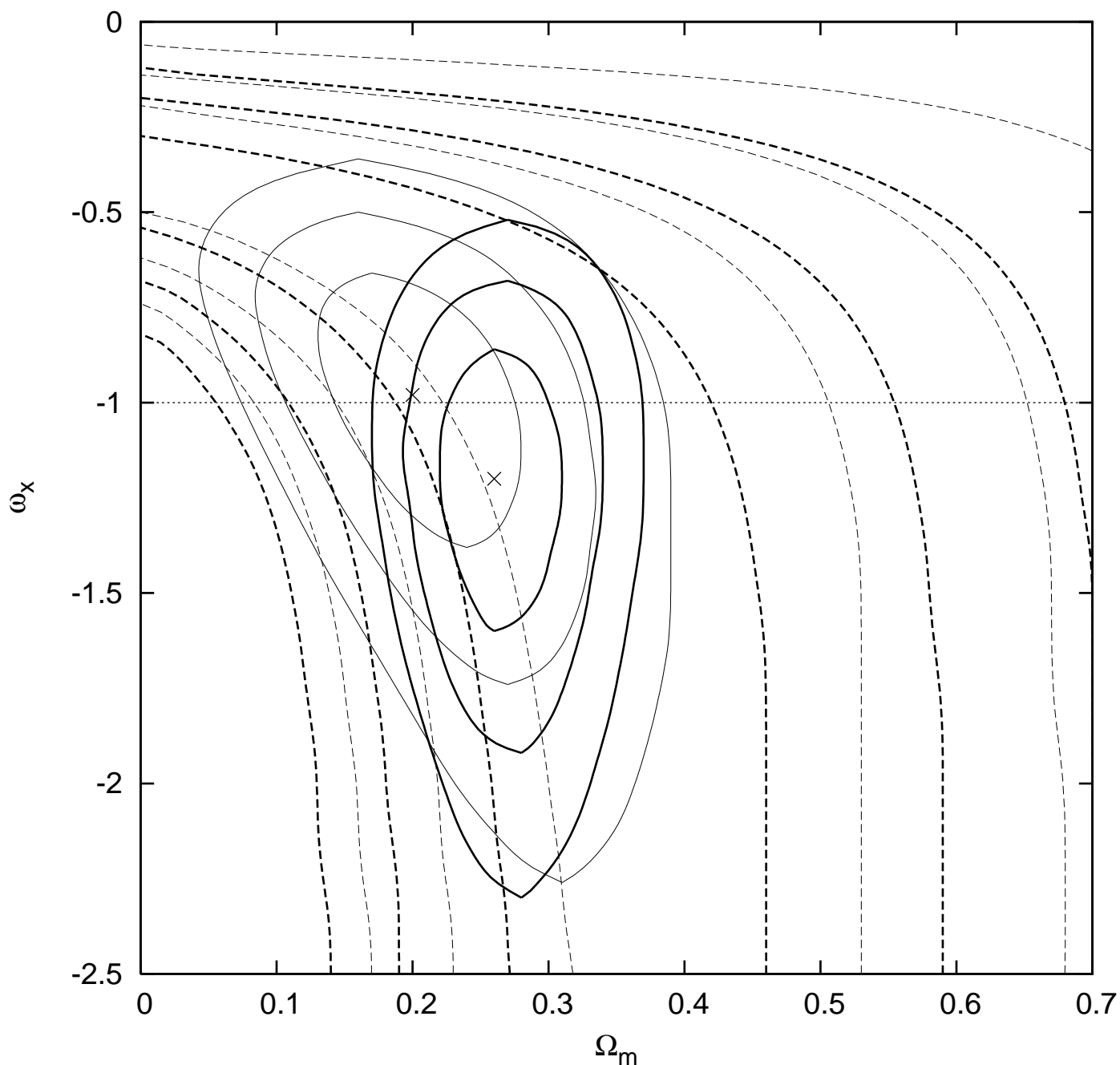
Fig. 2.— 1, 2, and 3 σ confidence level contours for the XCDM parametrization. Dashed lines denote constraints from Hubble parameter versus redshift data, while solid lines show the joint constraints (the crosses indicate the maximum likelihood points). The dotted horizontal line corresponds to spatially-flat ΛCDM models. Thick lines correspond to the $h = 0.73 \pm 0.03$ and $\Omega_\mathrm{b}h^2 = 0.022 \pm 0.0007$ priors (maximum likelihood is at $\Omega_\mathrm{m} = 0.26$ and $\omega_\mathrm{x} = -1.2$), while thin lines are for $h = 0.68 \pm 0.04$ and $\Omega_\mathrm{b}h^2 = 0.014 \pm 0.04$ (maximum likelihood is at $\Omega_\mathrm{m} = 0.20$ and $\omega_\mathrm{x} = -0.98$).
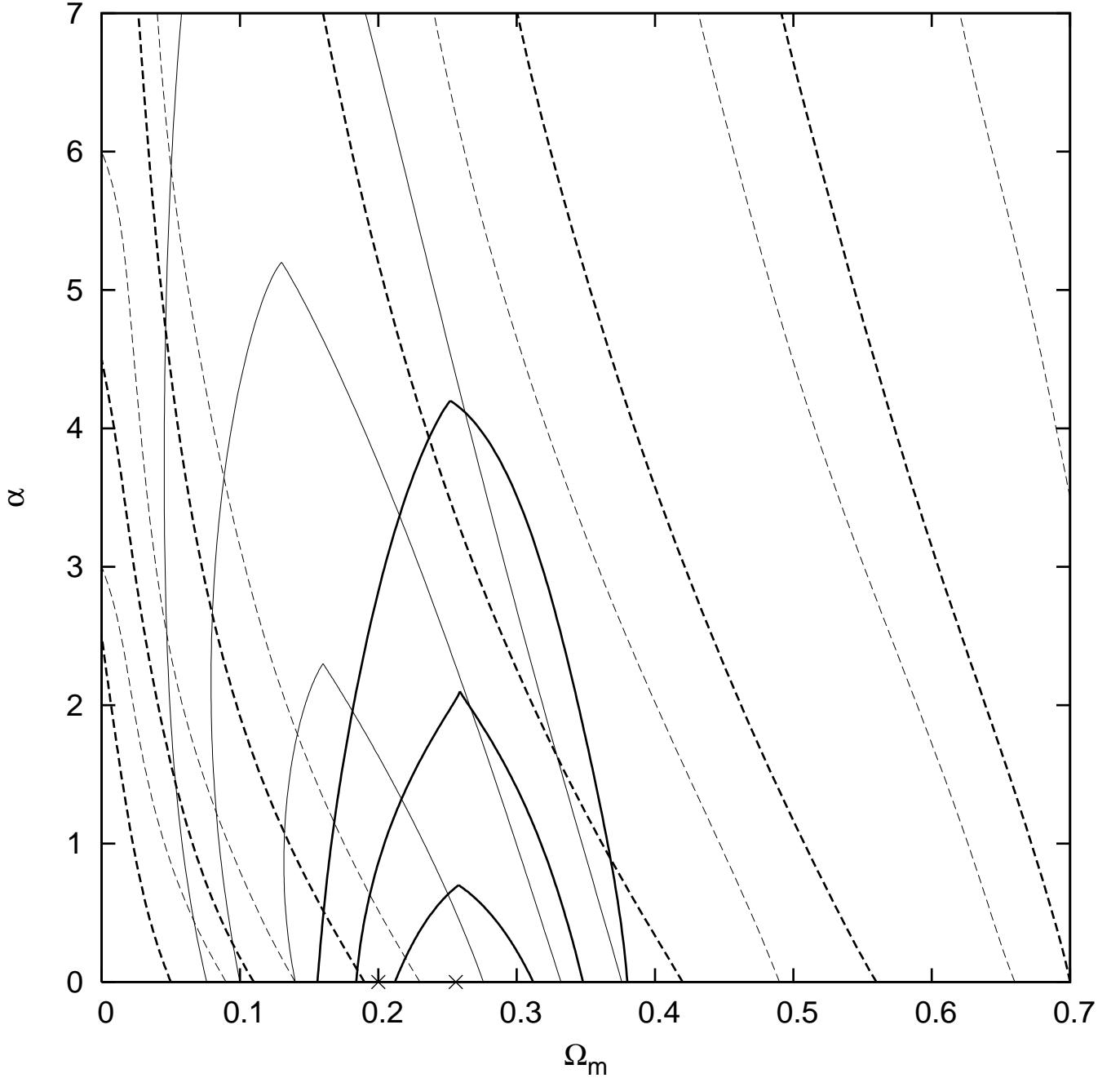
Fig. 3.— 1, 2, and 3 σ confidence level contours for the ϕCDM model. Dashed lines denote constraints from Hubble parameter versus redshift data, while solid lines show the joint constraints (the crosses on the horizontal axis indicate the maximum likelihood points). The horizontal $\alpha = 0$ axis corresponds to spatially-flat ΛCDM models. Thick lines correspond to the $h = 0.73 \pm 0.03$ and $\Omega_b h^2 = 0.022 \pm 0.0007$ priors (maximum likelihood is at $\Omega_m = 0.26$ and $\alpha = 0$), while thin lines are for $h = 0.68 \pm 0.04$ and $\Omega_b h^2 = 0.014 \pm 0.04$ (maximum likelihood is at $\Omega_m = 0.20$ and $\alpha = 0$).